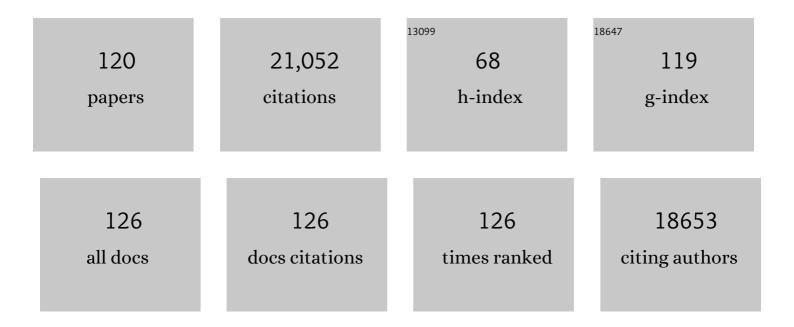
List of Publications by Year in descending order

Source: https://exaly.com/author-pdf/9362769/publications.pdf Version: 2024-02-01



#	Article	IF	CITATIONS
1	Donor–Acceptor Modification of Carbon Nitride for Enhanced Photocatalytic Hydrogen Evolution. Advanced Sustainable Systems, 2023, 7, .	5.3	14
2	An electrochemically reconstructed WC/WO <sub>2</sub> –WO <sub>3</sub> heterostructure as a highly efficient hydrogen oxidation electrocatalyst. Journal of Materials Chemistry A, 2022, 10, 622-631.	10.3	15
3	CsPbBr3 perovskite based tandem device for CO2 photoreduction. Chemical Engineering Journal, 2022, 443, 136447.	12.7	8
4	Promoting intramolecular charge transfer of graphitic carbon nitride by donor–acceptor modulation for visibleâ€light photocatalytic H <sub>2</sub> evolution. , 2022, 1, 294-308.		92
5	Advances in designing heterojunction photocatalytic materials. Chinese Journal of Catalysis, 2021, 42, 710-730.	14.0	182
6	All-organic Z-scheme photoreduction of CO2 with water as the donor of electrons and protons. Applied Catalysis B: Environmental, 2021, 285, 119773.	20.2	19
7	Light-driven directional ion transport for enhanced osmotic energy harvesting. National Science Review, 2021, 8, nwaa231.	9.5	24
8	Dual synergetic catalytic effects boost hydrogen electric oxidation performance of Pd/W18O49. Nano Research, 2021, 14, 2441-2450.	10.4	15
9	An Inorganic/Organic Sâ€Scheme Heterojunction H <sub>2</sub> â€Production Photocatalyst and its Charge Transfer Mechanism. Advanced Materials, 2021, 33, e2100317.	21.0	528
10	Ultra-Thin Carbon-Doped Bi2WO6 Nanosheets for Enhanced Photocatalytic CO2 Reduction. Transactions of Tianjin University, 2021, 27, 338-347.	6.4	29
11	A 3D Hierarchical Ti <sub>3</sub> C <sub>2</sub> T <sub>x</sub> /TiO <sub>2</sub> Heterojunction for Enhanced Photocatalytic CO <sub>2</sub> Reduction. ChemNanoMat, 2021, 7, 910-915.	2.8	14
12	Ultrathin 2D/2D Graphdiyne/Bi <sub>2</sub> WO <sub>6</sub> Heterojunction for Gas-Phase CO <sub>2</sub> Photoreduction. ACS Applied Energy Materials, 2021, 4, 8734-8738.	5.1	23
13	Solar-Driven Glucose Isomerization into Fructose via Transient Lewis Acid–Base Active Sites. ACS Catalysis, 2021, 11, 12170-12178.	11.2	36
14	Potassium/oxygen co-doped polymeric carbon nitride for enhanced photocatalytic CO2 reduction. Applied Surface Science, 2021, 563, 150310.	6.1	18
15	"Environmental phosphorylation―boosting photocatalytic CO2 reduction over polymeric carbon nitride grown on carbon paper at air-liquid-solid joint interfaces. Chinese Journal of Catalysis, 2021, 42, 1667-1676.	14.0	33
16	Nanocages of Polymeric Carbon Nitride from Lowâ€Temperature Supramolecular Preorganization for Photocatalytic CO <sub>2</sub> Reduction. Solar Rrl, 2020, 4, 1900469.	5.8	38
17	Two-dimensional gersiloxenes with tunable band gap as new photocatalysts. Rare Metals, 2020, 39, 610-612.	7.1	14
18	Enhanced photochemical CO <sub>2</sub> reduction in the gas phase by graphdiyne. Journal of Materials Chemistry A, 2020, 8, 7671-7676.	10.3	52

#	Article	IF	CITATIONS
19	A New Conducting Polymer with Exceptional Visibleâ€Light Photocatalytic Activity Derived from Barbituric Acid Polycondensation. Advanced Materials, 2020, 32, e1907702.	21.0	20
20	A Single Cu-Center Containing Enzyme-Mimic Enabling Full Photosynthesis under CO <sub>2</sub> Reduction. ACS Nano, 2020, 14, 8584-8593.	14.6	166
21	Designing a 0D/2D Sâ€Scheme Heterojunction over Polymeric Carbon Nitride for Visibleâ€Light Photocatalytic Inactivation of Bacteria. Angewandte Chemie, 2020, 132, 5256-5263.	2.0	14
22	Designing a 0D/2D Sâ€5cheme Heterojunction over Polymeric Carbon Nitride for Visibleâ€Light Photocatalytic Inactivation of Bacteria. Angewandte Chemie - International Edition, 2020, 59, 5218-5225.	13.8	822
23	Improving Artificial Photosynthesis over Carbon Nitride by Gas–Liquid–Solid Interface Management for Full Lightâ€Induced CO <sub>2</sub> Reduction to C <sub>1</sub> and C <sub>2</sub> Fuels and O <sub>2</sub> . ChemSusChem, 2020, 13, 1730-1734.	6.8	59
24	Controlling defects in crystalline carbon nitride to optimize photocatalytic CO <sub>2</sub> reduction. Chemical Communications, 2020, 56, 5641-5644.	4.1	83
25	MnCo Oxides Supported on Carbon Fibers for High-Performance Supercapacitors. Wuli Huaxue Xuebao/ Acta Physico - Chimica Sinica, 2020, 36, 1907072-0.	4.9	16
26	2D/2D FeNi-LDH/g-C <sub>3</sub> N <sub>4</sub> Hybrid Photocatalyst for Enhanced CO <sub>2</sub> Photoreduction. Wuli Huaxue Xuebao/ Acta Physico - Chimica Sinica, 2020, .	4.9	10
27	Photocatalysts based on polymeric carbon nitride for solar-to-fuel conversion. Interface Science and Technology, 2020, 31, 475-507.	3.3	2
28	Highly Selective CO2 Capture and Its Direct Photochemical Conversion on Ordered 2D/1D Heterojunctions. Joule, 2019, 3, 2792-2805.	24.0	189
29	Ni-P cluster modified carbon nitride toward efficient photocatalytic hydrogen production. Chinese Journal of Catalysis, 2019, 40, 867-874.	14.0	73
30	Designing Defective Crystalline Carbon Nitride to Enable Selective CO <sub>2</sub> Photoreduction in the Gas Phase. Advanced Functional Materials, 2019, 29, 1900093.	14.9	254
31	2D/2D Heterojunction of Ultrathin MXene/Bi <sub>2</sub> WO <sub>6</sub> Nanosheets for Improved Photocatalytic CO <sub>2</sub> Reduction. Advanced Functional Materials, 2018, 28, 1800136.	14.9	1,157
32	Effect of sacrificial agents on the dispersion of metal cocatalysts for photocatalytic hydrogen evolution. Applied Surface Science, 2018, 442, 361-367.	6.1	33
33	Dependence of Exposed Facet of Pd on Photocatalytic H <sub>2</sub> -Production Activity. ACS Sustainable Chemistry and Engineering, 2018, 6, 6478-6487.	6.7	41
34	Photocatalysis: Single-Atom Engineering of Directional Charge Transfer Channels and Active Sites for Photocatalytic Hydrogen Evolution (Adv. Funct. Mater. 32/2018). Advanced Functional Materials, 2018, 28, 1870224.	14.9	6
35	Singleâ€Atom Engineering of Directional Charge Transfer Channels and Active Sites for Photocatalytic Hydrogen Evolution. Advanced Functional Materials, 2018, 28, 1802169.	14.9	287
36	Hierarchical hollow cages of Mn-Co layered double hydroxide as supercapacitor electrode materials. Applied Surface Science, 2017, 413, 35-40.	6.1	98

#	Article	IF	CITATIONS
37	From Millimeter to Subnanometer: Vapor–Solid Deposition of Carbon Nitride Hierarchical Nanostructures Directed by Supramolecular Assembly. Angewandte Chemie, 2017, 129, 8546-8550.	2.0	16
38	Trace-level phosphorus and sodium co-doping of g-C 3 N 4 for enhanced photocatalytic H 2 production. Journal of Power Sources, 2017, 351, 151-159.	7.8	205
39	Facet effect of Pd cocatalyst on photocatalytic CO 2 reduction over g-C 3 N 4. Journal of Catalysis, 2017, 349, 208-217.	6.2	332
40	From Millimeter to Subnanometer: Vapor–Solid Deposition of Carbon Nitride Hierarchical Nanostructures Directed by Supramolecular Assembly. Angewandte Chemie - International Edition, 2017, 56, 8426-8430.	13.8	90
41	Cu2(OH)2CO3 clusters: Novel noble-metal-free cocatalysts for efficient photocatalytic hydrogen production from water splitting. Applied Catalysis B: Environmental, 2017, 205, 104-111.	20.2	137
42	Ultra-thin nanosheet assemblies of graphitic carbon nitride for enhanced photocatalytic CO <sub>2</sub> reduction. Journal of Materials Chemistry A, 2017, 5, 3230-3238.	10.3	621
43	A comparison study of alkali metal-doped g-C3N4 for visible-light photocatalytic hydrogen evolution. Chinese Journal of Catalysis, 2017, 38, 1981-1989.	14.0	244
44	Recent Advances in Morphology Control and Surface Modification of Bi-Based Photocatalysts. Wuli Huaxue Xuebao/ Acta Physico - Chimica Sinica, 2016, 32, 2841-2870.	4.9	85
45	Carbon-based H2-production photocatalytic materials. Journal of Photochemistry and Photobiology C: Photochemistry Reviews, 2016, 27, 72-99.	11.6	252
46	Corrosion mechanism of E-glass of chemical resistance glass fiber in acid environment. Journal Wuhan University of Technology, Materials Science Edition, 2016, 31, 872-876.	1.0	13
47	Synthesis of Organized Layered Carbon by Selfâ€Templating of Dithiooxamide. Advanced Materials, 2016, 28, 6727-6733.	21.0	59
48	Room-temperature synthesis of BiOI with tailorable (0 0 1) facets and enhanced photocatalytic activity. Journal of Colloid and Interface Science, 2016, 478, 201-208.	9.4	74
49	Size- and shape-dependent catalytic performances of oxidation and reduction reactions on nanocatalysts. Chemical Society Reviews, 2016, 45, 4747-4765.	38.1	568
50	Shape-dependent photocatalytic hydrogen evolution activity over a Pt nanoparticle coupled g-C <sub>3</sub> N <sub>4</sub> photocatalyst. Physical Chemistry Chemical Physics, 2016, 18, 19457-19463.	2.8	190
51	TiO2 nanosheets with exposed {001} facets for photocatalytic applications. Nano Research, 2016, 9, 3-27.	10.4	327
52	Au/PtO nanoparticle-modified g-C 3 N 4 for plasmon-enhanced photocatalytic hydrogen evolution under visible light. Journal of Colloid and Interface Science, 2016, 461, 56-63.	9.4	169
53	Microwave-assisted solvothermal synthesis of Bi4O5I2 hierarchical architectures with high photocatalytic performance. Catalysis Today, 2016, 264, 221-228.	4.4	100
54	Structure effect of graphene on the photocatalytic performance of plasmonic Ag/Ag2CO3-rGO for photocatalytic elimination of pollutants. Applied Catalysis B: Environmental, 2016, 181, 71-78.	20.2	219

#	Article	IF	CITATIONS
55	Supramolecular Chemistry in Molten Sulfur: Preorganization Effects Leading to Marked Enhancement of Carbon Nitride Photoelectrochemistry. Advanced Functional Materials, 2015, 25, 6265-6271.	14.9	89
56	Spectroscopy Applied to Engineering Materials. Journal of Spectroscopy, 2015, 2015, 1-2.	1.3	1
57	Polymeric Photocatalysts Based on Graphitic Carbon Nitride. Advanced Materials, 2015, 27, 2150-2176.	21.0	3,046
58	Dual Z-scheme charge transfer in TiO2–Ag–Cu2O composite for enhanced photocatalytic hydrogen generation. Journal of Materiomics, 2015, 1, 124-133.	5.7	86
59	A "uniform―heterogeneous photocatalyst: integrated p–n type CuInS <sub>2</sub> /NaInS <sub>2</sub> nanosheets by partial ion exchange reaction for efficient H <sub>2</sub> evolution. Chemical Communications, 2015, 51, 9381-9384.	4.1	22
60	Efficient photocatalytic reduction of CO2 by amine-functionalized g-C3N4. Applied Surface Science, 2015, 358, 350-355.	6.1	229
61	3D BiOl–GO composite with enhanced photocatalytic performance for phenol degradation under visible-light. Ceramics International, 2015, 41, 3511-3517.	4.8	74
62	Semiconductor-based photocatalytic CO <sub>2</sub> conversion. Materials Horizons, 2015, 2, 261-278.	12.2	380
63	Improving photocatalytic hydrogen production of metal–organic framework UiO-66 octahedrons by dye-sensitization. Applied Catalysis B: Environmental, 2015, 168-169, 572-576.	20.2	252
64	g-C3N4 modified TiO2 nanosheets with enhanced photoelectric conversion efficiency in dye-sensitized solar cells. Journal of Power Sources, 2015, 274, 77-84.	7.8	241
65	Selective photocatalytic decomposition of formic acid over AuPd nanoparticle-decorated TiO 2 nanofibers toward high-yield hydrogen production. Applied Catalysis B: Environmental, 2015, 162, 204-209.	20.2	107
66	Enhanced photocatalytic activity and stability of Z-scheme Ag2CrO4-GO composite photocatalysts for organic pollutant degradation. Applied Catalysis B: Environmental, 2015, 164, 380-388.	20.2	483
67	Development and Fabrication of Advanced Materials for Energy and Environment Applications 2014. Journal of Nanomaterials, 2014, 2014, 1-2.	2.7	0
68	Microwave-assisted heating synthesis: a general and rapid strategy for large-scale production of highly crystalline g-C <sub>3</sub> N <sub>4</sub> with enhanced photocatalytic H <sub>2</sub> production. Green Chemistry, 2014, 16, 4663-4668.	9.0	166
69	Rational Synthesis of Triangular Au–Ag <sub>2</sub> S Hybrid Nanoframes with Effective Photoresponses. Chemistry - A European Journal, 2014, 20, 2742-2745.	3.3	22
70	Solar-to-fuels conversion over In2O3/g-C3N4 hybrid photocatalysts. Applied Catalysis B: Environmental, 2014, 147, 940-946.	20.2	398
71	Noble-metal-free g-C3N4/Ni(dmgH)2 composite for efficient photocatalytic hydrogen evolution under visible light irradiation. Applied Surface Science, 2014, 319, 344-349.	6.1	169
72	Enhanced visible-light-driven photocatalytic hydrogen generation over g-C3N4 through loading the noble metal-free NiS2 cocatalyst. RSC Advances, 2014, 4, 6127.	3.6	136

#	Article	IF	CITATIONS
73	Direct evidence of plasmon enhancement on photocatalytic hydrogen generation over Au/Pt-decorated TiO <sub>2</sub> nanofibers. Nanoscale, 2014, 6, 5217-5222.	5.6	143
74	Enhanced photocatalytic CO2-reduction activity of electrospun mesoporous TiO2 nanofibers by solvothermal treatment. Dalton Transactions, 2014, 43, 9158.	3.3	105
75	Efficient CO <sub>2</sub> Capture and Photoreduction by Amineâ€Functionalized TiO <sub>2</sub> . Chemistry - A European Journal, 2014, 20, 10220-10222.	3.3	95
76	A strategy for in-situ synthesis of well-defined core–shell Au@TiO2 hollow spheres for enhanced photocatalytic hydrogen evolution. Chemical Engineering Journal, 2014, 257, 112-121.	12.7	51
77	Recent advances in visible light Bi-based photocatalysts. Chinese Journal of Catalysis, 2014, 35, 989-1007.	14.0	481
78	Two-dimensional layered composite photocatalysts. Chemical Communications, 2014, 50, 10768.	4.1	551
79	g-C <sub>3</sub> N <sub>4</sub> -Based Photocatalysts for Hydrogen Generation. Journal of Physical Chemistry Letters, 2014, 5, 2101-2107.	4.6	1,107
80	Vectorial doping-promoting charge transfer in anatase TiO2 {001} surface. Applied Surface Science, 2014, 319, 167-172.	6.1	55
81	Dye-sensitized Pt@TiO <sub>2</sub> core–shell nanostructures for the efficient photocatalytic generation of hydrogen. Beilstein Journal of Nanotechnology, 2014, 5, 360-364.	2.8	18
82	Effects of the preparation method on the structure and the visible-light photocatalytic activity of Ag <sub>2</sub> CrO <sub>4</sub> . Beilstein Journal of Nanotechnology, 2014, 5, 658-666.	2.8	76
83	Au@TiO <sub>2</sub> –CdS Ternary Nanostructures for Efficient Visible-Light-Driven Hydrogen Generation. ACS Applied Materials & Interfaces, 2013, 5, 8088-8092.	8.0	177
84	Ionâ€Induced Synthesis of Uniform Singleâ€Crystalline Sulphideâ€Based Quaternaryâ€Alloy Hexagonal Nanorings for Highly Efficient Photocatalytic Hydrogen Evolution. Advanced Materials, 2013, 25, 2567-2572.	21.0	45
85	Nanoparticle heterojunctions in ZnS–ZnO hybrid nanowires for visible-light-driven photocatalytic hydrogen generation. CrystEngComm, 2013, 15, 5688.	2.6	77
86	Artificial photosynthetic hydrogen evolution over g-C3N4 nanosheets coupled with cobaloxime. Physical Chemistry Chemical Physics, 2013, 15, 18363.	2.8	101
87	Large impact of heating time on physical properties and photocatalytic H2 production of g-C3N4 nanosheets synthesized through urea polymerization in Ar atmosphere. International Journal of Hydrogen Energy, 2013, 38, 13159-13163.	7.1	103
88	In-situ growth of CdS quantum dots on g-C3N4 nanosheets for highly efficient photocatalytic hydrogen generation under visible light irradiation. International Journal of Hydrogen Energy, 2013, 38, 1258-1266.	7.1	339
89	NiS2 Co-catalyst decoration on CdLa2S4 nanocrystals for efficient photocatalytic hydrogen generation under visible light irradiation. International Journal of Hydrogen Energy, 2013, 38, 7218-7223.	7.1	76
90	Red phosphor/g-C3N4 heterojunction with enhanced photocatalytic activities for solar fuels production. Applied Catalysis B: Environmental, 2013, 140-141, 164-168.	20.2	219

#	Article	IF	CITATIONS
91	Molecule-Based Water-Oxidation Catalysts (WOCs): Cluster-Size-Dependent Dye-Sensitized Polyoxometalates for Visible-Light-Driven O2 Evolution. Scientific Reports, 2013, 3, 1853.	3.3	69
92	Au/Pt Nanoparticle-Decorated TiO <sub>2</sub> Nanofibers with Plasmon-Enhanced Photocatalytic Activities for Solar-to-Fuel Conversion. Journal of Physical Chemistry C, 2013, 117, 25939-25947.	3.1	277
93	Surfactantâ€Free Subâ€2 nm Ultrathin Triangular Gold Nanoframes. Small, 2013, 9, 2880-2886.	10.0	66
94	Development and Fabrication of Advanced Materials for Energy and Environment Applications. Journal of Nanomaterials, 2013, 2013, 1-2.	2.7	8
95	Plasmon-Enhanced Hydrogen Evolution on Au-InVO4 Hybrid Microspheres. RSC Advances, 2012, 2, 5513.	3.6	40
96	Preparation of Au-BiVO <sub>4</sub> Heterogeneous Nanostructures as Highly Efficient Visible-Light Photocatalysts. ACS Applied Materials & Interfaces, 2012, 4, 418-423.	8.0	259
97	Mesoporous plasmonic Au–TiO2 nanocomposites for efficient visible-light-driven photocatalytic water reduction. International Journal of Hydrogen Energy, 2012, 37, 17853-17861.	7.1	151
98	In situ growth of Au nanoparticles on Fe2O3 nanocrystals for catalytic applications. CrystEngComm, 2012, 14, 7229.	2.6	48
99	Gold Coating of Silver Nanoprisms. Advanced Functional Materials, 2012, 22, 849-854.	14.9	116
100	Monodisperse α-Fe2O3 Mesoporous Microspheres: One-Step NaCl-Assisted Microwave-Solvothermal Preparation, Size Control and Photocatalytic Property. Nanoscale Research Letters, 2011, 6, 1.	5.7	452
101	Calcium phosphate drug nanocarriers with ultrahigh and adjustable drug-loading capacity: One-step synthesis, in situ drug loading and prolonged drug release. Nanomedicine: Nanotechnology, Biology, and Medicine, 2011, 7, 428-434.	3.3	47
102	Preparation, Characterization and Application of Hollow Microspheres Assembled with Nanocrystals of Iron Oxides. Wuji Cailiao Xuebao/Journal of Inorganic Materials, 2011, 26, 458-466.	1.3	2
103	Preparation and photocatalytic property of α-Fe2O3 hollow core/shell hierarchical nanostructures. Journal of Physics and Chemistry of Solids, 2010, 71, 1680-1683.	4.0	33
104	Preparation and Sustained-Release Property of Triblock Copolymer/Calcium Phosphate Nanocomposite as Nanocarrier for Hydrophobic Drug. Nanoscale Research Letters, 2010, 5, 781-785.	5.7	38
105	Calcium phosphate/block copolymer hybrid porous nanospheres: Preparation and application in drug delivery. Materials Letters, 2010, 64, 2299-2301.	2.6	21
106	Hierachically Nanostructured Mesoporous Spheres of Calcium Silicate Hydrate: Surfactantâ€Free Sonochemical Synthesis and Drugâ€Delivery System with Ultrahigh Drugâ€Loading Capacity. Advanced Materials, 2010, 22, 749-753.	21.0	142
107	Iron hydroxyl phosphate microspheres: Microwave-solvothermal ionic liquid synthesis, morphology control, and photoluminescent properties. Journal of Solid State Chemistry, 2010, 183, 1704-1709.	2.9	16
108	Rapid microwave-assisted synthesis and characterization of cellulose-hydroxyapatite nanocomposites in N,N-dimethylacetamide solvent. Carbohydrate Research, 2010, 345, 1046-1050.	2.3	38

#	Article	IF	CITATIONS
109	Hydrothermal synthesis of relatively uniform CePO4@LaPO4 one-dimensional nanostructures with highly improved luminescence. Journal of Alloys and Compounds, 2010, 492, 559-563.	5.5	14
110	Porous nanocomposites of PEG-PLA/calcium phosphate: room-temperature synthesis and its application in drug delivery. Dalton Transactions, 2010, 39, 4435.	3.3	37
111	ZnFe2O4 nanoparticles: Microwave-hydrothermal ionic liquid synthesis and photocatalytic property over phenol. Journal of Hazardous Materials, 2009, 171, 431-435.	12.4	149
112	Formation of γ-Fe2O3 hierarchical nanostructures at 500°C in a high magnetic field. Journal of Magnetism and Magnetic Materials, 2009, 321, 3057-3060.	2.3	31
113	Iron oxide hollow spheres: Microwave–hydrothermal ionic liquid preparation, formation mechanism, crystal phase and morphology control and properties. Acta Materialia, 2009, 57, 2154-2165.	7.9	104
114	Preparation and Drug Release Properties of Nanostructured CaCO <sub>3</sub> Porous Hollow Microspheres. Wuji Cailiao Xuebao/Journal of Inorganic Materials, 2009, 24, 166-170.	1.3	10
115	Hierarchically Nanostructured α-Fe <sub>2</sub> O <sub>3</sub> Hollow Spheres:  Preparation, Growth Mechanism, Photocatalytic Property, and Application in Water Treatment. Journal of Physical Chemistry C, 2008, 112, 6253-6257.	3.1	272
116	Hierarchically Nanostructured Magnetic Hollow Spheres of Fe <sub>3</sub> O <sub>4</sub> and γ-Fe <sub>2</sub> O <sub>3</sub> :  Preparation and Potential Application in Drug Delivery. Journal of Physical Chemistry C, 2008, 112, 1851-1856.	3.1	328
117	Nanostructured porous hollow ellipsoidal capsules of hydroxyapatite and calcium silicate: preparation and application in drug delivery. Journal of Materials Chemistry, 2008, 18, 2722.	6.7	166
118	Fe3O4 polyhedral nanoparticles with a high magnetization synthesized in mixed solvent ethylene glycol–water system. New Journal of Chemistry, 2008, 32, 1526.	2.8	86
119	Surfactant-Free Preparation and Drug Release Property of Magnetic Hollow Core/Shell Hierarchical Nanostructures. Journal of Physical Chemistry C, 2008, 112, 12149-12156.	3.1	118
120	SnO2 and ZnO Nanostructured Spheres Self-assembled by Nanocrystals: Microwave-assisted Preparation and Enhancement of Photocatalytic Activity. Chemistry Letters, 2008, 37, 1002-1003.	1.3	7